Ab Initio Study on Mechanisms and Kinetics for Reaction of NCS with NO

Hui-Lung Chen,*,† Rongshun Zhu,† Hsin-Tsung Chen,† Han-Jung Li,‡ and Shin-Pon Ju*,§

Cherry L. Emerson Center for Scientific Computation and Department of Chemistry, Emory University, Atlanta, Georgia 30322, Department of Chemistry, National Taiwan Normal University, 88, Section 4, Tingchow Road, Taipei 116, Taiwan, and Department of Mechanical and Electro-Mechanical Engineering, Center for Nanoscience and Nanotechnology, National Sun-Yat-Sen University Kaohsiung, Taiwan 804

Received: February 15, 2008; Revised Manuscript Received: March 21, 2008

The mechanisms and kinetics of the reaction of a thiocyanato radical (NCS) with NO were investigated by a high-level ab initio molecular orbital method in conjunction with variational RRKM calculations. The species involved were optimized at the B3LYP/6-311++G(3df,2p) level, and their single-point energies were refined by the CCSD(T)/aug-cc-PVQZ//B3LYP/6-311+G(3df,2p) method. Our calculated results indicate favorable pathways for the formation of several isomers of an NCSNO complex. Formation of OCS + N_2 also is possible, although this pathway involves a substantial energy barrier. The predicted total rate constants, k_{total}, at a 2 torr He pressure can be represented by the following equations: $k_{total} = 9.74 \times 10^{26} T^{-13.88} \exp(-6.53 \text{ (kcal mol}^{-1})/RT)$ at $T = 298-950$ K and $1.17 \times 10^{-22} T^{2.52} \exp(-6.86 \text{ (kcal mol}^{-1})/RT)$ at $T = 960-3000$ K, in units of cm^3 molecule^{-1} s^{-1}, and the predicted values are in good agreement with the experimental results in the temperature range of 298−468 K. The calculated results clearly indicate that the branching ratio for R_{M1} in the temperature range of 298−950 K has the largest value (R_{M1} accounts for 0.53−0.39). However, in the higher temperature range (960−3000 K), the formation of OCS + N_2 (**P5**) with branching ratio R_{P5} (0.40−0.79) becomes dominant. The rate constants for key individual product channels are provided for different temperature and pressure conditions.

1. Introduction

Since its first discovery in 1957 by Holland et al.,[1,2] the thiocyanato radical (NCS), as an isoelectronic species of the isocyanate radical (NCO), has been of interest to experimentalists and theorists. In 1968, Dixon and Ramsay[3] analyzed the absorption bands of NCS at 330 and 400 nm and assigned them to the $A^2\Pi$-$X^2\Pi$-X^2 transitions. In 1984, the laser-induced fluorescence (LIF) spectrum of NCS was observed and discussed by Ohtoshi et al.,[4] and they found the Fermi interaction between the 001 and 020 levels in the ground $X^2\Pi$ state. In addition, the NCS radical has been the topic of numerous spectroscopic studies,[5–9] and the spectrum is complex due to the presence of Renner−Teller and spin−orbit interactions. This radical may be a key intermediate in the combustion of sulfur-containing fuels and may play an important role in the RAPRENOx (rapid reduction of nitrogen oxides) process.[10,11]

Hershberger and Baren[12] carried out the first timed kinetic study of the NCS radical in 1999. They proposed some possible reaction channels and presented the following thermochemical information:

$$\text{NCS} + \text{NO} \rightarrow \text{N}_2\text{O} + \text{CS} \quad \Delta H = -7.7 \pm 1.4 \text{ kcal/mol} \quad \text{(a)}$$

$$\rightarrow \text{N}_2 + \text{OCS} \quad \Delta H = -127.4 \pm 0.8 \text{ kcal/mol} \quad \text{(b)}$$

$$\rightarrow \text{NCSNO} \quad \text{(c)}$$

They also performed kinetics experiments on the NCS + NO reaction over the temperature range of 298−468 K. The rate constants at low total pressures of around 2 He are represented by

$$k_{\text{NCS+NO}} = 4.1 \pm 1.4 \times 10^{-15} \exp(1.561 \pm 116/T) \text{ (cm}^3 \text{ molecule}^{-1} \text{ s}^{-1})$$

However, the diversity and complexity of such a reaction mechanism still could not be defined accurately. Hence, a detailed theoretical construction on the potential energy surface (PES) and the kinetic prediction of the NCS + NO reaction are very crucial. In this study, we carried out variational RRKM calculations based on energies and structures predicted by a high-level molecular orbital method.

2. Computational Methods

With the Gaussian 03 suite of programs[13] we performed molecular orbital calculations involving density-functional theory (DFT) with Becke's three-parameter (B3) exchange functional and the Lee−Yang−Parr (LYP) correlation functional (B3LYP)[14,15] with a 6-311++G(3df,2p) basis set. The calculated equilibrium structures (local minima and saddle points) were characterized with calculations of harmonic vibrational wavenumbers at the same level of theory, with calculations of intrinsic reaction coordinates (IRC)[16] to establish the link between transition structure and intermediates. To obtain reliable energies, we performed single-point calculations employing a coupled-cluster technique with single and double excitations and evaluations by perturbation theory of triple contributions CCSD(T)[17,18] based on the geometries optimized at the B3LYP/6-311++G(3df,2p) level. The highest level of theory attained in this work is thus denoted CCSD(T)/aug-cc-PVQZ//B3LYP/6-311++G(3df,2p). Unless otherwise specified, CCSD(T) single-point energies were used. The rate constants for key product channels were computed with the variational transition-state theory (VTST) and microcanonical RRKM theory[19–22] using the VariFlex[23] program.

* Corresponding authors. E-mail: (H.-L.C.) hlchen@euch4e.chem.emory.edu and (S.-P.J.) jushin-pon@mail.nsysu.edu.tw.
† Emory University.
‡ National Taiwan Normal University.
§ National Sun-Yat-Sen University Kaohsiung.

10.1021/jp8013805 CCC: $40.75 © 2008 American Chemical Society
Published on Web 05/16/2008

TABLE 1: Geometries (Bond Lengths and Angles), EA of NCS Molecule Calculated at Various Levels of Theory, and Some Experimental Data from the Literature

level of theory	N−C (Å)	C−S (Å)	EA[a] (eV)
MP2/6-31++G(d,p)	1.15	1.68	
MP2/6-311++G(3df,2p)	1.15	1.66	
B3LYP/6-31++G(d,p)	1.19	1.64	
B3LYP/6-311++G(3df,2p)	1.17	1.63	3.46
CCSD(T)/aug-cc-PVTZ//B3LYP/6-311++G(3df,2p)			3.45
CCSD(T)/aug-cc-PVQZ//B3LYP/6-311++G(3df,2p)			3.52
CCSD(T)/aug-cc-PV5Z//B3LYP/6-311++G(3df,2p)			3.54
experiment	1.16[b]	1.63[b]	3.51[c]

[a] Energy difference between anion NCS^- and neutral NCS. [b] Refs 3 and 24. [c] Ref 25.

3. Results and Discussion

3.1. Computational Condition Tests. In Table 1, we present data for the electron affinities (EA) and geometrical parameters of the NCS molecule calculated at various levels of theory with pertinent experimental data from the literature. The N−C and C−S bond lengths predicted by the hybrid density functional B3LYP method with a 6-311++G(3df,2p) basis set were 1.17 and 1.63 Å, which are in satisfactory agreement with experimental values (1.16 and 1.63 Å, respectively),[3,24] whereas the calculated B3LYP energy for the electron affinity of NCS, 3.46 eV, substantially underestimated the experimental value (3.51, shown in Table 1).[25] In this regard, we performed a single-point energy calculation at the CCSD(T)/aug-cc-PVQZ level, based on the geometries obtained from B3LYP/6-311++G(3df,2p) and derived a satisfactory result, 3.52 eV, which is much closer to the experimental value. In addition, we also employed the same method to calculate the ionization energy of the NO molecule, and the calculated value, $IE_{(NO)} = 9.23$ eV, is in good agreement with the experimental data (9.263 ± 0.011 eV).[26] For this reason, we therefore chose CCSD(T)/aug-cc-PVQZ//B3LYP/6-311++G(3df,2p) as the method for an energetic calculation of all feasible processes in the reaction system NCS + NO.

3.2. PES for NCS + NO Reaction. As depicted in Scheme 1, we classified the examined reaction into five paths, **A**−**E**, corresponding to five possible product channels. The intermediates are correspondingly numbered **IM1**−**IM5**, and the products in these five channels, CS + NON, CS + ONS, CS + c-NNO, CS + N_2O, and OCS + N_2, are labeled in the same order of **P1**−**P5**. **TS1**−**TS8** denotes a transition-state species connecting two intermediates located at local minima.

The computed geometric structures of the local minima and transition-state structures at the B3LYP/6-311++G(3df,2p) level are shown in Figure 1. The profiles of the PES calculated at the CCSD(T)/aug-cc-PVQZ//B3LYP/6-311++G(3df,2p) level are shown in Figure 2.

All the calculated energetics for reactants, intermediates, transition states, and products are listed in Table 2, among which the zero-point vibrational energy (ZPE) correction is considered, and the energies with respect to the reactant (NCS + NO) calculated at the CCSD(T) level are denoted as CRE.

As shown in Figure 2, our calculated results for channels **A** and **B** are **R** → **IM1** → **TS2** → **P1** and **R** → **IM1** → **P2**, respectively. The energy barrier in the former path via **TS2** is 108.5 kcal/mol with respect to the reactants (NCS + NO), with an overall endothermicity of 107.5 kcal/mol, forming the products of CS + NON (**P1**). **IM1** and **IM2** can directly produce the final products CN + ONS (**P2**) via two variational transition states with an endothermicity of 59.0 kcal/mol. Besides, it was found that there exist two possible orientations for N−N bond addition, and these two separated adducts, **IM3** and **IM4**, lead to completely different follow-up reaction mechanisms and different product formations. First, with regard to channel **C**, **R** → **IM3** → **TS4** → **P3**, the first step is the barrierless formation of **IM3**, a long-lived intermediate with an exothermicity of 17.0 kcal/mol. It may go through a dissociative transition state, **TS4**, lying 67.1 kcal/mol above the reactants, and form the products of CS + c-NNO (**P3**), with an overall endothermicity of 58.7 kcal/mol. Second, for the other possible route to generate **P4**, **R** → **IM4** → **TS6** → **P4**, the formation of the **IM4** conformer is barrierless with an exothermicity of 14.1 kcal/mol. It then takes 22.5 kcal/mol, via **TS6**, to form eventual products (CS + N_2O, **P4**) by the breaking of the C−N bond (the C−N bond length in **TS6** is 1.773 Å), and this process is exothermic by 4.0 kcal/mol. Third, in contrast to the formation of **P4**, the **IM4** adduct will proceed by another pathway, via **TS7** ($E_a = 10.3$ kcal/mol with respect to the reactants), to form a four-membered ring intermediate, **IM5**, and then go further by passing a small barrier (**TS8**, 2.1 kcal/mol) to open the ring by breaking two C−N and O−N bonds simultaneously and forming the products of OCS + N_2 (**P5**), with an overall exothermicity of 124.8 kcal/mol. Consequently, our calculated results thus show the major possible reaction pathway in NCS + NO to be channel **E**, **R** → **IM4** → **TS7** → **IM5** → **TS8** → **P5**, which is also the thermochemically most favorable.

In addition, we also attempted to evaluate the accuracy of the calculated relative energies since there is some discrepancy between calculated and experimental exothermicities for CS + N_2O (**P4**) and OCS + N_2 (**P5**) of ∼3 to ∼4 kcal/mol. Further calculations were performed to extrapolate the CCSD(T) results to the complete basis set limit. By fitting results obtained from basis sets with different n values, aug-cc-PVnZ, an extrapolation to $n \rightarrow \infty$ can be achieved. For this purpose, the cardinal number X is introduced, where $X = 2$, 3, 4, and 5 for $n =$ D, T, Q, and 5, respectively. For extrapolations to the complete basis set limit, we used the two-parameter exponential model[28] $E = a + bX^{-3}$ to fit the data points. As shown in Table 2, the result is quite consistent; the discrepancy between CCSD(T)/aug-cc-PVQZ and CCSD(T)/aug-cc-PVnZ ($n \rightarrow \infty$) is less than 0.7 kcal/mol. Moreover, a number of different composite methods were employed for comparison, including G3B3,[29] CBS-QB3,[30] and W1U,[31] which are listed in Table S1. Interestingly, similar to the CCSD(T)/aug-cc-PVQZ results, the computed relative energies for the products of CS + N_2O (**P4**) and OCS + N_2 (**P5**) at these levels are all up-shifted by ∼2 to ∼4 kcal/mol as compared to experimental values. Therefore, the deviation might come from the experimental results. Checking the experimental data,[9] one can see that ΔH_f (NCS) has an ∼4.0 kcal/mol difference based on different measurements. We used the authors' recommended upper limit value ($\Delta H_f \leq 72.7 \pm 0.8$)[9] for comparison in this work, which may lead to the overestimation of experimental exothermicities for the products of CS + N_2O (**P4**) and OCS + N_2 (**P5**).

3.3. Fukui Function Analysis. From the aforementioned results, it was found that the NCS + NO reaction may first form the four primary adducts—**IM1**, **IM2**, **IM3**, and

SCHEME 1: Schematic Diagram of Proposed Paths for NCS + NO Reaction

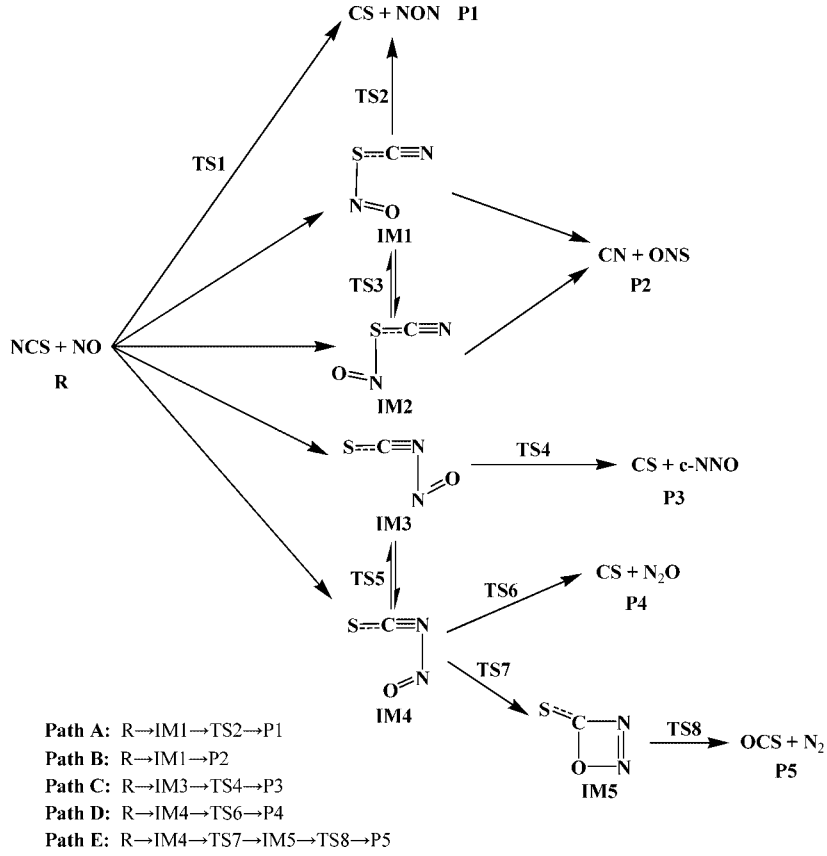

IM4—which are energetically more stable than the reactants by 24.5, 22.7, 17.0, and 14.1 kcal/mol, respectively. Obviously, the former two adducts, **IM1** and **IM2**, possess a much higher stability than that of **IM3** and **IM4**. Concerning this phenomenon, we calculated the Fukui functions[32,33] and applied the theory of hard-and-soft acid-and-base (HSAB) to seek the possible explanation. The extrapolation of the general behavior "soft likes soft" and "hard likes hard" locally, together with the idea that the larger the value of the Fukui function, the greater the reactivity, is also a very useful approach to explain the chemical reactivity of many chemical systems.[34–39] Clearly, the determination of the specific sites at which the interaction between two chemical species is going to occur is of fundamental importance to the determination of the path and the products of a given reaction. Gázquez and Meńdez[40] also stated that the largest value of the Fukui function is, in general, associated with the most reactive site. In our calculation for N electrons in a system, independent calculations are made for the corresponding $(N - 1)$, N, and $(N + 1)$ electron systems with the same geometry. A natural population analysis yields $q_k(N - 1)$, $q_k(N)$, and $q_k(N + 1)$ for the predicted possible sites of reaction of NCS and NO molecules, and the Fukui function is calculated as a difference of population between N and $N + 1$ or N and $N - 1$ electron systems. We choose the f^0 value for comparison because the NCS + NO reaction is more characteristic of a radical reaction.[33] According to our calculated data in Table 3, it was found that the largest Fukui function (f^0, 0.676) is on the S atom in the NCS radical and that of the other reactant NO is on the N atom (0.628), which accounts for the formation of the complexes (**IM1** and **IM2**) being more effective than other complexes (such as **IM3** and **IM4**). In addition, applying the HSAB theory, we find also that the largest values for the local softness s^0 for both reactants are on the S atom of NCS and the N atom of NO (2.201 and 1.949), which also accounts for the favorable formation of the adducts of **IM1** and **IM2**. In contrast, the Fukui function was calculated to be smallest ($f^0 = 0.372$), and the local softness ($s^0 = 1.155$) of the O atom in NO was found, indicating an unfavorable addition through its O-terminus site, which readily was explained.

3.4. Rate Constant Calculation. Variational TST and RRKM calculations carried out for this reaction with the VariFlex code including the more favorable reaction channels are shown as the following Scheme 2:

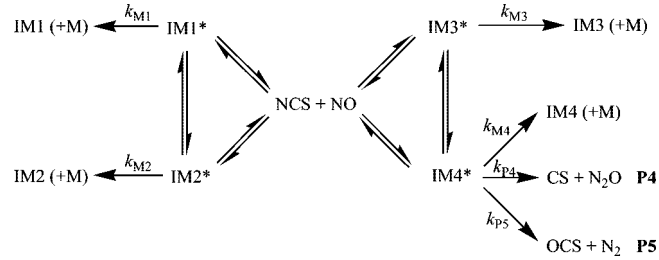

The reverse dissociation of the energized intermediates **IM1**−**IM4** back to the reactants was included in our kinetic calculations. The energies used in the calculation are plotted in Figure 2, and the vibrational frequencies and moments of inertia are listed in Table S2. The Lennard-Jones (LJ) parameters employed for the NCS + NO reaction are as follows: for He,[41] $\sigma = 2.55$ Å and $\varepsilon/k = 10.0$ K and for NCSNO, $\sigma = 3.90$ Å and $\varepsilon/k = 205.0$ K, which are approximated to be the same as the analogous study of the

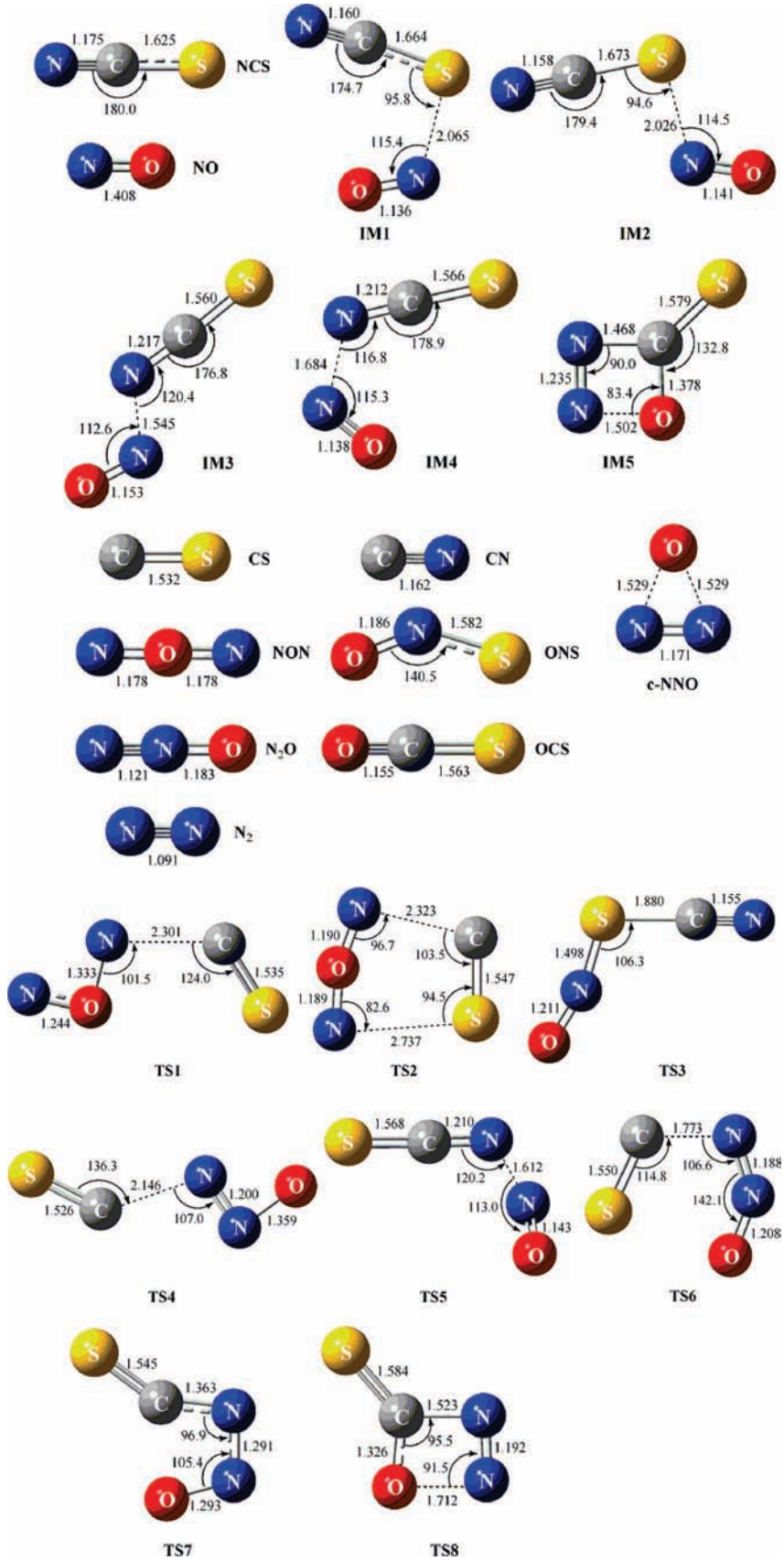

Figure 1. Optimized geometries of relevant reactants, intermediates, transition states, and products on PESs of NCS + NO reactions, calculated at the B3LYP/6-311++G(3df,2p) level. Bond lengths are in angstroms and angles in degrees.

NCO + NO system.[42] For the variational rate constant calculations using the VariFlex code, a statistical treatment of the transitional mode contributions to the transition-state partition functions was performed variationally. The number of states was evaluated according to the variable reaction coordinate flexible transition-state theory;[23,43] an energy grain

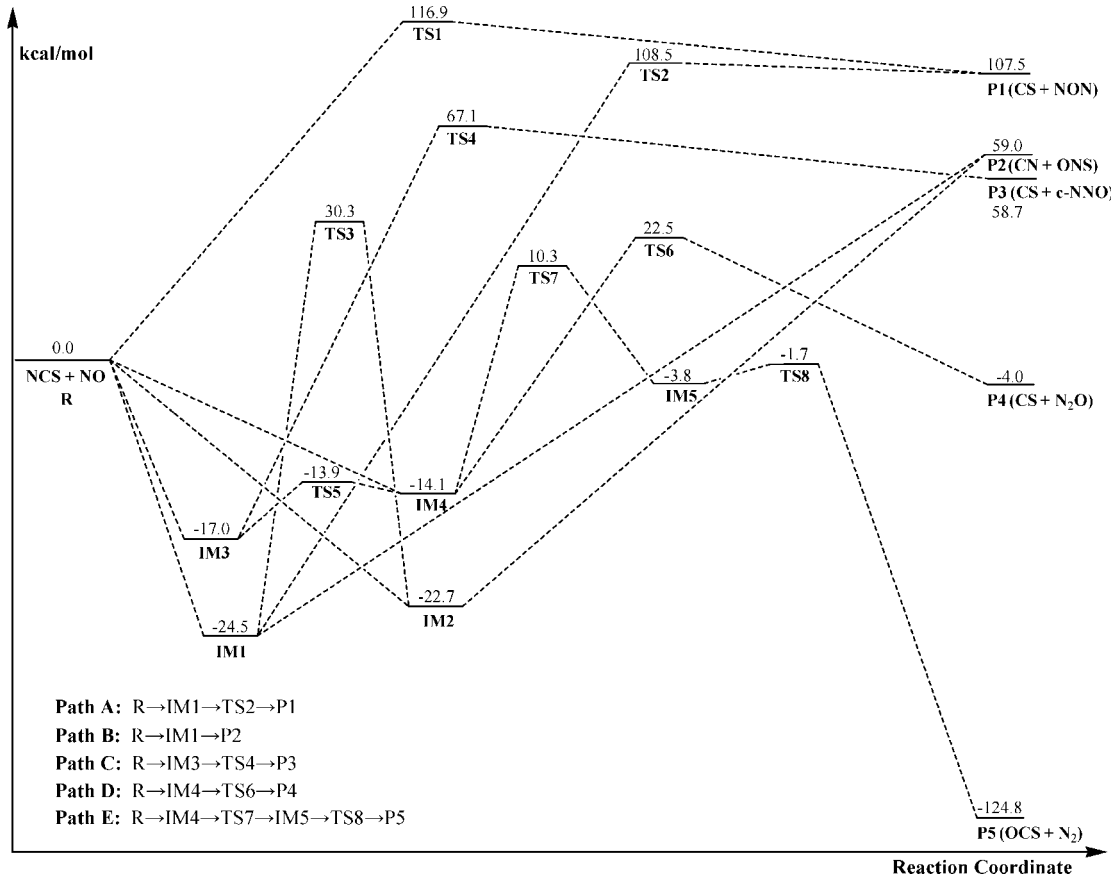

Figure 2. Calculated profiles of PES for possible paths in NCS + NO reaction at the CCSD(T)/aug-cc-PVQZ//B3LYP/6-311++G(3df,2p) level; labels represent the same species as those in Scheme 1.

TABLE 2: ZPE (Hartree), Total Energy (TE, Hartree), and Relative Energies (RE, kcal/mol) of Reactant, Intermediates, Transition States, and Products, Calculated at the B3LYP/6-311++G(3df,2p) (BTE) and CCSD(T)/aug-cc-PVQZ//B3LYP/6-311++G(3df,2p) (CTE and CRE) Levels for Reaction of NCS + NO

species	ZPE[a]	BTE + ZPE[b]	CTE + ZPE[b]	CRE[c]	experiment[d]
R (NCS + NO)	0.012608	−620.979513	−620.168119	0.0	
IM1	0.015641	−621.013655	−620.207120	−24.5	
IM2	0.015472	−621.011424	−620.204309	−22.7	
IM3	0.015858	−621.009552	−620.195180	−17.0	
IM4	0.015667	−621.003388	−620.190505	−14.1	
IM5	0.016813	−620.972816	−620.174196	−3.8	
TS1	0.009919	−620.737139	−619.981808	116.9	
TS2	0.013453	−620.788709	−619.995179	108.5	
TS3	0.014238	−620.933158	−620.119895	30.3	
TS4	0.011207	−620.857954	−620.061219	67.1	
TS5	0.015495	−621.002036	−620.190242	−13.9	
TS6	0.014882	−620.934973	−620.132238	22.5	
TS7	0.015687	−620.956496	−620.151670	10.3	
TS8	0.015264	−620.972154	−620.170752	−1.7	
P1 (CS + NON)	0.012555	−620.793083	−619.996832	107.5	
P2 (CN + ONS)	0.011688	−620.884416	−620.074101	59.0	
P3 (CS + c-NNO)	0.009947	−620.867358	−620.074654	58.7	
P4 (CS + N_2O)	0.014184	−620.976600	−620.174478	−4.0 (−4.4)[e]	≥(−7.7 ± 1.4)
P5 (OCS + N_2)	0.014818	−621.168315	−620.366936	−124.8 (−125.5)[e]	≥(−127.4 ± 0.8)

[a] ZPE (au) at the B3LYP/6-311++G(3df,2p) level. [b] Unit of energy is hartree. [c] Relative energy (kcal/mol) with respect to reactants. [d] Thermochemical information is obtained from standard tables (ref 27), except for NCS, where the value of $\Delta H_f \leq 72.7 \pm 0.8$ kcal/mol (ref 9) is used. [e] Relative energy with respect to reactants at CCSD(T)/aug-cc-PVnZ//B3LYP/6-311++G(3df,2p) level with an extrapolation to $n \rightarrow \infty$.

size of 1.00 cm^{-1} was used for the convolution of the conserved mode vibrations, and a grain size of 80.00 cm^{-1} was used for the generation of the transitional mode numbers of states. The estimate of the transitional mode contribution to the transition-state number of states for a given energy was evaluated via Monte Carlo integration with 10 000 configuration numbers. The energy-transfer process was computed on the basis of the exponential down model with an $\langle \Delta E \rangle_{down}$ value (the mean energy transferred per collision) of 100 cm^{-1} for He. To achieve convergence in the integration over the energy range, an energy grain size of 120 cm^{-1} was used. The total angular momentum J covered the range from 1 to 250 in steps of 10 for the E,J-resolved calculation.

TABLE 3: Condensed Fukui Functions for N, C, and S Atoms in NCS; N and O Atoms in NO; and Global and Local Softness of Molecules Calculated at the B3LYP/6-311++G(3df,2p) Level

	f^{0a}					local softness $(s^0)^b$			
molecule	N	O	C	S	global softness $(S)^c$	N	O	C	S
NO	0.628	0.372			3.104	1.949	1.155		
NCS	0.378		0.054	0.676	3.256	1.231		0.176	2.201

[a] Atomic charges according to natural population analysis. [b] $S^0 = f^0 S$. [c] $S = 1/(\mathrm{IE} - \mathrm{EA})$; energy unit is hartrees.

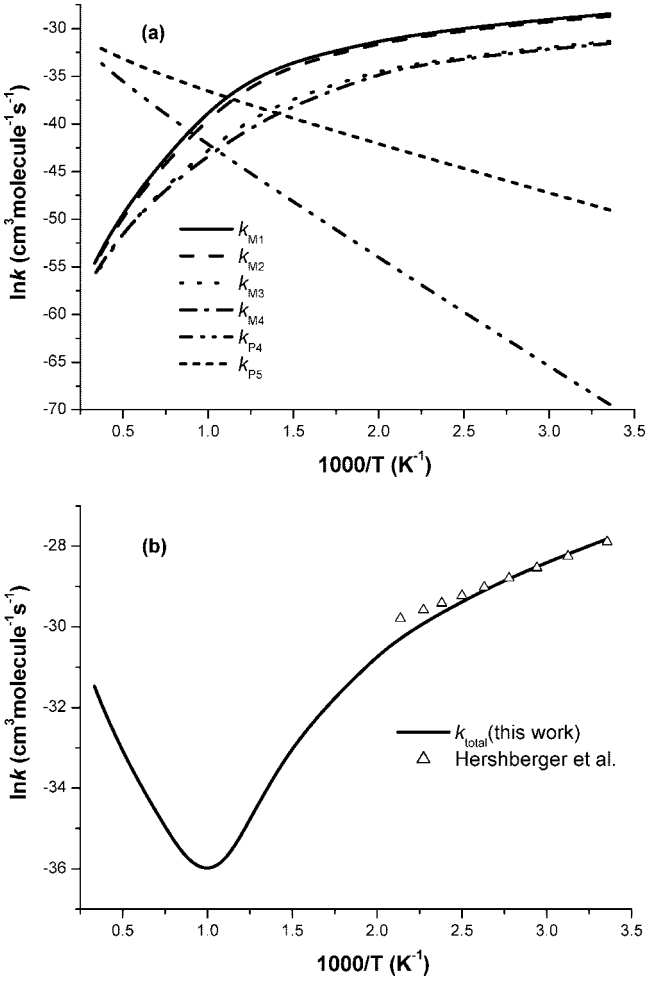

Figure 3. Predicted rate constants of k_{M1}, k_{M2}, k_{M3}, k_{M4}, k_{P4}, and k_{P5} (a) and comparison of total rate constants ($k_{total} = k_{M1} + k_{M2} + k_{M3} + k_{M4} + k_{P4} + k_{P5}$) with experimental values at He pressures of 2 torr in the temperature range of 298−3000 K. Δ: Ref 12.

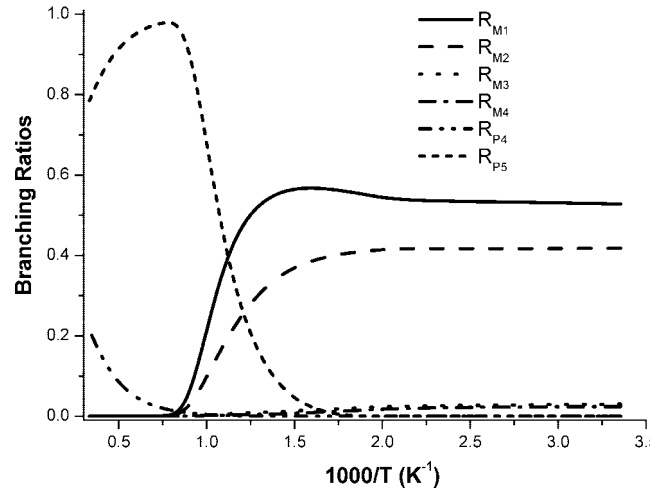

Figure 4. Predicted branching ratios for primary reaction channels of NCS + NO at 2 torr of He pressure in the temperature range of 298−3000 K.

In the RRKM calculations, we neglected the pathways of **P1**−**P3** formation since their energy barriers are much higher than **TS7**, in which **TS7** is the rate-controlling step of our proposed most predominant channel. The predicted values for k_{M1}, k_{M2}, k_{M3}, k_{M4}, k_{P4}, and k_{P5} and the comparison of the total rate constants ($k_{total} = k_{M1} + k_{M2} + k_{M3} + k_{M4} + k_{P4} + k_{P5}$) with the experimental values at He pressures of 2 torr in the temperature range of 298−3000 K are shown in Figure 3a,b, respectively. It can be seen that the values of k_{M1}, k_{M2}, k_{M3}, and k_{M4} substantially decrease when the temperature increases from 700 to 3000 K. However, the values of k_{P4} and k_{P5} have a positive temperature dependence in the whole temperature range. In addition, it can be seen from Figure 3b that our predicted values (solid line) are in good agreement with experimental results (measured by Hershberger and Baren[12]) in the temperature range of 298−468 K, although there is some discrepancy at higher temperatures. The branching ratios for the six primary reaction channels (R_{M1}, R_{M2}, R_{M3}, R_{M4}, R_{P4}, and R_{P5}) at a He pressure of 2 torr in the temperature range of 298−3000 K are shown in Figure 4. It clearly shows that the branching ratio for R_{M1} in the temperature range of 298−950 K possess the largest values (R_{M1} accounts for 0.53−0.39). However, in the higher temperature range (960−3000 K), the branching ratio for R_{P5} (0.40−0.79), which forms OCS + N_2 (**P5**), becomes the most significant product. Moreover, it was found also that the formation of CS + N_2O (**P4**) turned somewhat competitive when the temperature went higher than 1400 K. Therefore, the calculated results demonstrate that the formation of the OCS + N_2 (**P5**) product from the NCS + NO reaction is the dominant reaction channel under the circumstance of higher temperature.

We summarized the rate expressions (k_{M1}, k_{M2}, k_{M3}, k_{M4}, k_{P4}, and k_{P5}) at five specific pressures between 2 torr and 50 atm in the temperature range of 298−3000 K, which are listed in Table 4. As we can see, in this temperature range, the values of k_{M1}, k_{M2}, k_{M3}, and k_{M4} have a strong pressure dependence; however, there is pressure independence for values of k_{P4} and k_{P5}. The predicted total rate constants, k_{total}, at a 2 torr of He pressure can be represented as $k_{total} = 9.74 \times 10^{26} T^{-13.88} \exp(-6.53\ (\mathrm{kcal\ mol^{-1}})/RT)$ at $T = 298-950$ K and $1.17 \times 10^{-22} T^{2.52} \exp(-6.86\ (\mathrm{kcal\ mol^{-1}})/RT)$ at $T = 960-3000$ K, respectively, in units of $\mathrm{cm^3\ molecule^{-1}\ s^{-1}}$. At present, no comparison can be made for the experimental data when the temperatures are higher than 468 K. For this newly identified, potentially important, prompt NO precursor reaction, our results are recommended for high-temperature combustion modeling applications.

4. Conclusion

The mechanisms and kinetics for the NCS + NO reaction were studied with a high-level CCSD(T) method. The total and individual rate constants for the primary channels of the aforementioned reactions in the temperature range of 298−3000

TABLE 4: Predicted Rate Expressions[a] of k_{M1}, k_{M2}, k_{M3}, k_{M4}, k_{P4}, and k_{P5} at He pressures of 2, 380, and 760 torr and 10 and 50 atm in the Temperature Range of 298−3000 K

reaction	*P*	*A*	*n*	*B*
k_{M1}	2 torr	1.21×10^{38}	−17.68	−9.13
	380 torr	1.03×10^{40}	−17.84	−9.76
	760 torr	3.11×10^{40}	−17.89	−9.97
	10 atm	2.17×10^{42}	−18.11	−10.93
	50 atm	6.33×10^{43}	−18.31	−11.88
k_{M2}	2 torr	7.45×10^{35}	−17.10	−8.11
	380 torr	6.64×10^{37}	−17.26	−8.73
	760 torr	2.09×10^{38}	−17.32	−8.93
	10 atm	1.60×10^{40}	−17.55	−9.88
	50 atm	5.37×10^{41}	−17.77	−10.83
k_{M3}	2 torr	1.41×10^{26}	−14.51	−5.00
	380 torr	8.49×10^{27}	−14.63	−5.38
	760 torr	2.30×10^{28}	−14.66	−5.51
	10 atm	9.12×10^{29}	−14.82	−6.06
	50 atm	2.04×10^{31}	−15.00	−6.67
k_{M4}	2 torr	3.98×10^{21}	−13.19	−3.24
	380 torr	1.32×10^{23}	−13.24	−3.38
	760 torr	3.36×10^{23}	−13.27	−3.46
	10 atm	1.45×10^{25}	−13.44	−4.00
	50 atm	3.64×10^{26}	−13.63	−4.61
k_{P4}	2 torr	5.72×10^{-20}	1.85	−21.11
	380 torr	5.72×10^{-20}	1.85	−21.11
	760 torr	5.72×10^{-20}	1.85	−21.11
	10 atm	5.72×10^{-20}	1.85	−21.11
	50 atm	5.72×10^{-20}	1.85	−21.11
k_{P5}	2 torr	7.43×10^{-20}	1.72	−8.73
	380 torr	7.43×10^{-20}	1.72	−8.73
	760 torr	7.43×10^{-20}	1.72	−8.73
	10 atm	7.43×10^{-20}	1.72	−8.73
	50 atm	7.43×10^{-20}	1.72	−8.73

[a] Rate constants are represented by $k = AT^n \exp(B \text{ (kcal mol}^{-1})/RT)$ in units of cm^3 molecule^{-1} s^{-1}.

K were predicted. The four association adducts, **IM1**−**IM4**, are dominant in the low-temperature range ($T = 298-950$ K); over 950 K, the formation of OCS + N_2 (**P5**) is the primary channel through the PESs of the NCS + NO reaction. Our predicted total and individual rate constants and product branching ratios for this critical reaction may be employed for combustion kinetic modeling applications.

Acknowledgment. S.-P.J. thanks the National Science Council of the Republic of China for supporting this study, under Grant NSC-096-2628-E-110-005-MY2.

Supporting Information Available: Table S1: total and relative energies for products of CS + N_2O and OCS + N_2, calculated at different levels of theory. Table S2: frequencies and moments of inertia for species involved in reaction of NCS + NO, calculated at the B3LYP/6-311++G(3df,2p) level. This material is available free of charge via the Internet at http://pubs.acs.org.

Note Added after ASAP Publication. This article was released ASAP on May 16, 2008. Scheme 2 has been revised. The correct version posted on May 24, 2008.

References and Notes

(1) Holland, R. Ph.D. Thesis, University of London, London, U.K., 1957.
(2) Holland, R.; Style, D. W. G.; Dixon, R. N.; Ramsay, D. A. *Nature (London, U.K.)* **1958**, *182*, 336.
(3) Dixon, R. N.; Ramsay, D. A. *Can. J. Phys.* **1968**, *46*, 2619.
(4) Ohtoshi, H.; Tsukiyama, K.; Yanagibori, A.; Shibuya, K.; Obi, K.; Tanaka, K. *Chem. Phys. Lett.* **1984**, *111*, 136.
(5) Northrup, F. J.; Sears, T. J. *Chem. Phys. Lett.* **1985**, *159*, 421.
(6) Northrup, F. J.; Sears, T. J. *Mol. Phys.* **1990**, *71*, 45.
(7) Tokue, I.; Kobayashi, K.; Honda, T.; Ito, Y. *J. Phys. Chem.* **1990**, *94*, 3485.
(8) Northrup, F. J.; Sears, T. J. *J. Chem. Phys.* **1990**, *93*, 2337.
(9) Ruscic, B.; Berkowitz, J. *J. Chem. Phys.* **1994**, *101*, 7975.
(10) Perry, R. A.; Siebers, D. L. *Nature (London, U.K.)* **1986**, *324*, 657.
(11) Miller, J. A.; Bowman, C. T. *Int. J. Chem. Kinet.* **1991**, *23*, 289.
(12) Baren, R. E.; Hershberger, J. F. *J. Phys. Chem. A* **1999**, *103*, 11340.
(13) Frisch, M. J.; Trucks, G. W.; Schlegel, H. B.; Scuseria, G. E.; Robb, M. A.; Cheeseman, J. R.; Montgomery, J. A., Jr.; Vreven, T.; Kudin, K. N.; Burant, J. C.; Millam, J. M.; Iyengar, S. S.; Tomasi, J.; Barone, V.; Mennucci, B.; Cossi, M.; Scalmani, G.; Rega, N.; Petersson, G. A.; Nakatsuji, H.; Hada, M.; Ehara, M.; Toyota, K.; Fukuda, R.; Hasegawa, J.; Ishida, M.; Nakajima, T.; Honda, Y.; Kitao, O.; Nakai, H.; Klene, M.; Li, X.; Knox, J. E.; Hratchian, H. P.; Cross, J. B.; Adamo, C.; Jaramillo, J.; Gomperts, R.; Stratmann, R. E.; Yazyev, O.; Austin, A. J.; Cammi, R.; Pomelli, C.; Ochterski, J. W.; Ayala, P. Y.; Morokuma, K.; Voth, G. A.; Salvador, P.; Dannenberg, J. J.; Zakrzewski, V. G.; Dapprich, S.; Daniels, A. D.; Strain, M. C.; Farkas, O.; Malick, D. K.; Rabuck, A. D.; Raghavachari, K.; Foresman, J. B.; Ortiz, J. V.; Cui, Q.; Baboul, A. G.; Clifford, S.; Cioslowski, J.; Stefanov, B. B.; Liu, G.; Liashenko, A.; Piskorz, P.; Komaromi, I.; Martin, R. L.; Fox, D. J.; Keith, T.; Al-Laham, M. A.; Peng, C. Y.; Nanayakkara, A.; Gill, P. M. W.; Challacombe, M.; Johnson, B.; Chen, W.; Wong, M. W.; Gonzalez, C.; Pople, J. A. *Gaussian 03, revision D.02*; Gaussian, Inc.: Wallingford, CT, 2004.
(14) (a) Becke, A. D. *J. Chem. Phys.* **1993**, *98*, 5648. (b) Becke, A. D. *J. Chem. Phys.* **1992**, *96*, 2155. (c) Becke, A. D. *J. Chem. Phys.* **1992**, *97*, 9173.
(15) Lee, C.; Yang, W.; Parr, R. G. *Phys. Rev. B: Condens. Matter Mater. Phys.* **1988**, *37*, 785.
(16) Gonzalez, C.; Schlegel, H. B. *J. Phys. Chem.* **1989**, *90*, 2154.
(17) Lee, T. J.; Scuseria, G. In *Quantum-Mechanical Electronic Structure Calculations with Chemical Accuracy*; Langhoff, S. F., Ed.; Kluwer: Dordrecht, The Netherlands, 1995.
(18) Knowles, P. J.; Hampel, C.; Werner, H.-J. *J. Chem. Phys.* **1993**, *99*, 5219.
(19) Klippenstein, S. J.; Marcus, R. A. *J. Chem. Phys.* **1987**, *87*, 3410.
(20) Klippenstein, S. J. *J. Chem. Phys.* **1992**, *96*, 367.
(21) Wardlaw, D. M.; Marcus, R. A. *Chem. Phys. Lett.* **1984**, *110*, 230.
(22) Wardlaw, D. M.; Marcus, R. A. *J. Chem. Phys.* **1985**, *83*, 3462.
(23) Klippenstein, S. J.; Wagner, A. F.; Dunbar, R. C.; Wardlaw, D. M.; Robertson, S. H. *VariFlex: version 1.00*; 1999.
(24) Ouazbir, M.; Chambaud, G.; Rosmus, P.; Knowles, P. J. *Phys. Chem. Chem. Phys.* **1999**, *1*, 2649.
(25) Dillard, J. G.; Franklin, J. L. *J. Chem. Phys.* **1968**, *48*, 2353.
(26) Kuo, S.-C.; Zhang, Z.; Ross, S. K.; Klemm, R. B. *J. Phys. Chem. A* **1997**, *101*, 4035.
(27) Chase, M. W.; Davies, C. A.; Downey, J. R.; Frurip, D. J.; McDonald, R. A.; Syverud, A. N. *J. Phys. Chem. Ref. Data* **1985**, *14*, 1.
(28) Helgaker, T.; Klopper, W.; Koch, H.; Noga, J. *J. Chem. Phys.* **1997**, *106*, 9639.
(29) Baboul, A. G.; Curtiss, L. A.; Redfern, P. C.; Raghavachari, K. *J. Chem. Phys.* **1999**, *110*, 7650.
(30) (a) Montgomery, J. A., Jr.; Frisch, M. J.; Ochterski, J. W.; Petersson, G. A. *J. Chem. Phys.* **1999**, *110*, 2822. (b) Montgomery, J. A., Jr.; Frisch, M. J.; Ochterski, J. W.; Petersson, G. A. *J. Chem. Phys.* **2000**, *112*, 6532.
(31) (a) Martin, J. M. L.; de Oliveira, G. *J. Chem. Phys.* **1999**, *111*, 1843. (b) Parthiban, S.; Martin, J. M. L. *J. Chem. Phys.* **2001**, *114*, 6014.
(32) Parr, R. G.; Yang, W. *J. Am. Chem. Soc.* **1984**, *106*, 4049.
(33) Yang, W.; Mortier, W. J. *J. Am. Chem. Soc.* **1986**, *108*, 5708.
(34) Nguyen, M. T.; Chandra, A. K.; Sakai, S.; Morokuma, K. *J. Org. Chem.* **1999**, *64*, 65.
(35) Nguyen, L. T.; Proft, F. D.; Chandra, A. K.; Uchimaru, T.; Nguyen, M. T.; Geerlings, P. *J. Org. Chem.* **2001**, *66*, 6096.
(36) Lŏpez, P.; Meńdez, F. *Org. Lett.* **2004**, *6*, 1781.
(37) Lin, Y.-l.; Lee, Y.-m.; Lim, C. *J. Am. Chem. Soc.* **2005**, *127*, 11336.
(38) Chen, H.-L.; Wu, C.-W.; Ho, J.-J. *J. Phys. Chem. A* **2006**, *110*, 8893.
(39) Chen, H.-L.; Li, H.-J.; Ho, J.-J. *Chem. Phys. Lett.* **2007**, *442*, 35.
(40) Gázquez, J. L.; Meńdez, F. *J. Phys. Chem.* **1994**, *98*, 4591.
(41) Hippler, H.; Troe, J.; Wendelken, H. J. *J. Chem. Phys.* **1983**, *78*, 6709.
(42) Zhu, R. S.; Lin, M. C. *J. Phys. Chem. A* **2000**, *104*, 10807.
(43) Gilbert, R. G.; Smith, S. C. *Theory of Unimolecular and Recombination Reactions*; Blackwell Scientific: Oxford, 1990.

JP8013805